ACS APPLIED MATERIALS & INTERFACES

Research Article

www.acsami.org

Functionalized Polysilsesquioxane-Based Hybrid Silica Solid Amine Sorbents for the Regenerative Removal of CO_2 from Air

Kochukunju Adisser Saraladevi Abhilash,* Thomas Deepthi, Retnakumari Amma Sadhana, and K. George Benny

Analytical and Spectroscopy Division, Analytical Spectroscopy and Ceramics Group, Propellants, Polymers, Chemicals and Materials Entity, Vikram Sarabhai Space Centre, Trivandrum 695022, Kerala, India

Supporting Information

ABSTRACT: Functionalized polysilsesquioxane-based hybrid silica materials are presented as solid amine sorbents for direct CO_2 capture from air. The sorbent was synthesized from amine and vinyl functionalized alkoxysilanes by a simple, energy efficient, and cost-effective co-condensation method. The material, containing bound amine functionalities, was found to have a selective CO_2 capturing capacity of 1.68 mmol/g from atmospheric air with an adsorption half time of 50 min. This material also showed a maximum adsorption capacity of 2.28 mmol/g in pure CO_2 and 1.92 mmol/g in 10% CO_2. Desorption started at a temperature as low as 60 °C, and complete desorption occurred at 80 °C. The sorbent exhibited high recycling ability, and 100 cycles of adsorption/desorption were demonstrated in pure CO_2 and 50 cycles in ambient air without any loss in efficiency.

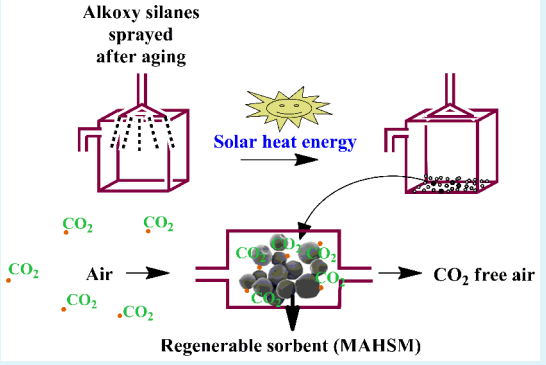

KEYWORDS: *silanes, silsesquioxanes, CO_2, adsorption, desorption*

1. INTRODUCTION

The feasibility of CO_2 capture from atmospheric air to control the increasing CO_2 levels has been under active discussion in the past decade. Many researchers[1,2] advocated for direct capture of CO_2 from air to reduce atmospheric CO_2 level and believed that it is closer to geoengineering than to conventional mitigation by industrial effluent gas treatment. The "Air as the renewable carbon source" thought was discussed by Olah et al.[3] At the same time, a suitable material to remove CO_2, regeneratively, from an ultradilute environment-like atmospheric air on a large scale is challenging and is still in its infancy. The most familiar materials include CaO,[4] $(CaOH)_2$,[5] NaOH,[6] etc., which absorb CO_2 by chemisorption, and regeneration is energy intensive. Zeolites[7,8] and activated carbons[9,10] adsorb through physisorption but are less selective. Zeolites require high regeneration temperature, and their performance is adversely affected by humidity. Metal organic frameworks (MOFs)[11−15] are making good impact, and recent developments[16−18] are highly promising toward CO_2 capture from dilute environments. Functionalized porous polymers[19−21] also form an important class of materials being investigated as promising candidates for CO_2 removal.

Amine-based solid sorbents[22−26] which hold CO_2 by chemisorption have been extensively studied in the past several years as materials for CO_2 capture. Amine species can be either immobilized by wet impregnation or grafted onto the porous substrates[24−33] like silica, activated carbon, and polymers for use as regenerable systems for CO_2 removal. Most of the research articles published on mesoporous sorbents, especially mesoporous silica with high surface area and optimum amine loading, show high CO_2 removal efficiency[28,29] from pure CO_2, but CO_2 capture studies from atmospheric air are lacking. Polyethylenimine-based silica systems were studied for air capture by many investigators.[30−33]The higher CO_2 removal capability of amine-impregnated sorbents gets faded by the problem of loss in efficiency after successive regeneration cycles.[3,28,29,34−36] To overcome amine loss observed in amine-impregnated sorbents, aminosilanes are covalently grafted on to the intrachannel surface of mesoporous silica either through post-modification or by direct synthesis (co-condensation). Though several reports exist for the synthesis of amine-grafted silica for CO_2 capture using post-modification of silica with organosilanes,[7,37−40] only some of them were reported for direct capture of CO_2 from air. Triamine-grafted pore expanded mesoporous silica (TRI-PE-MCM-41) was reported by Sayari and co-workers[41,42] with a CO_2 capture capacity of 0.98 mmol/g at low CO_2 concentration, and also the effect of humidity[43] on CO_2 adsorption of amine containing sorbents was studied. Subsequently, a breakthrough in this field was made by Jones and co-workers[44] by making HAS (hyperbranched amino silica) sorbent using in situ ring opening polymerization of aziridine. However, synthesis of mesoporous silica (SBA-15, MCM-41, etc.) is energy intensive as it requires calcination at temperature as high as 550 °C for 5−6 h.

Received: May 28, 2015
Accepted: July 21, 2015
Published: July 21, 2015

DOI: 10.1021/acsami.5b04674
ACS Appl. Mater. Interfaces 2015, 7, 17969−17976

Direct synthesis via hydrolysis and co-condensation of organosilanes with aminosilanes in the presence of an organic template using acid or base catalyst produces amine functionalized mesoprous silica materials. However, only a few amine functionalized co-condensed silica materials were reported for CO_2 adsorption studies.[38,45−47] Polysilsesquioxanes are relatively new to the class of amine sorbents and remain less explored for CO_2 capture. Mesoporous amine bridged polysilsesquioxane was reported by Qi et al.[48] and organic−inorganic polyaspartimide involving polyhedral oligomeric silsesquioxane by Shanmugham et al.[49] for CO_2 removal application. Formation of fully condensed polyhedral oligomeric silsesquioxane by hydrolytic condensation of trifunctional organosilicon monomers was discussed by Voronkov and Lavrent'yev,[50] and they reported that octamers with ethyl and vinyl groups are formed in alcoholic media without the addition of a catalyst. Methods exist for preparing functionalized hybrid silica materials[51] and surface functionalized polysilsesquioxane hard spheres,[52] but these materials were not evaluated for CO_2 adsorption properties.

Synthesis of polysilsesquioxane-based hybrid silica materials for CO_2 capture from air is reported here, and the use of such materials for this application is new to the best of our knowledge. Optimization strategy for producing these sorbents in good yield and with maximum CO_2 adsorption, performance of the sorbent in different CO_2 partial pressures, and recycling capability of the sorbent are explored in detail.

2. EXPERIMENTAL SECTION

2.1. Materials. 3-Aminopropyl triethoxysilane (99%) and vinyl triethoxysilane (97%) were purchased from Sigma-Aldrich, and absolute alcohol was from Merck Millipore, India, and used as such without any further purification.

2.2. Synthesis of Sorbent. 3-Aminopropyl triethoxysilane (AS, 30.4579 g) and vinyl triethoxysilane (VS, 26.2090 g) were mixed in absolute ethanol/water mixture so that the molar concentration of silane/ethanol/water in the mixture is 1:30:8. The mixture was stirred for 3 h and aged in a closed vessel at ambient temperature for 5 days. After aging, the system was diluted by adding 5 L of ethanol, shaken well, sprayed on to glass plates using a spray gun, and kept under sunlight. The material that formed was vacuum-dried at 85 °C for 1 h. Yield: 17.2 g. The material was designated as MAHSM (monoamine-based hybrid silica material).

2.3. Characterization. Elemental analysis was performed using PerkinElmer 2400 CHNS analyzer with a thermal conductivity detector. The morphology of the sample was obtained through field emission scanning electron microscopy (FE-SEM, JEOL Microscope JSM 6060). Microstructure of the sample was evaluated using transmission electron microscope model FEI (Tecnai G2 30 S-TWIN) with an accelerating voltage of 300 kV. For TEM measurements, the sample dispersed in acetone was drop-casted on the carbon-coated copper grid and dried in vacuum at room temperature before observation. Infrared spectra of the samples were recorded using PerkinElmer Spectrum GX A FTIR spectrometer in the wavelength region 4000−400 cm^{-1} with a spectral resolution of 4 cm^{-1} by making a pellet with dry KBr. Solid-state ^{13}C and ^{29}Si NMR experiments were performed using a Bruker AVANCE 400 spectrometer (9.4 T), operating at Larmor frequencies of 100.6 and 79.5 MHz, respectively, equipped with a Bruker cross-polarization magic angle spinning (CP-MAS) probe and 4 mm ZrO_2 rotors, spinning at 5 kHz. For ^{13}C, the $^{1}H-^{13}C$ CP-MAS pulse sequence was employed with optimized contact time of 2 ms and a repetition time (D1) of 5 s. ^{29}Si MAS NMR spectra were acquired by using $^{1}H-^{29}Si$ cross-polarization (CP-MAS) with contact time of 5 ms. Adamantane was used as the external references for ^{13}C (methine resonance at 38.5 ppm) and peak of tetrakis(trimethylsilyl)silane (TTMS) at −9.8 ppm for ^{29}Si NMR measurements.

XRD measurements were carried out by a Bruker D8-Discover X-ray diffractometer operating with a Cu anode (40 kV, 40 mA) keeping the sample on a zero background Si sample cup. Diffractograms were recorded using Lynx Eye solid-state detector from 5° to 50° at a step size 0.02° and time/step 0.5 s. TG-MS analysis was done using PerkinElmer Pyris 1 TGA coupled with Clarus SQ8T quadruple mass spectrometer through a heated fused silica transfer line. The transfer line temperature was maintained at 210 °C, and the evolved species were ionized in electron impact ionization mode with electron energy of 70 eV. Mass spectra of the evolved species were recorded for a mass range 10−500 amu. Thermogravimetric analyses were done with PerkinElmer Pyris 1 thermogravimetric analyzer in inert atmosphere (helium), with heating rate of 10 °C/min. The heat of absorption of CO_2 was obtained from differential scanning calorimetry (DSC) technique using TA Instrument DSC Q20 maintaining isothermal conditions and measuring heat flow to or from the sample cell. The absorption was performed in a flow of pure CO_2 (100 mL/min) at 30 °C. The heat of adsorption was calculated by integrating heat flow over the time period of adsorption. Raman imaging was performed using Witec Alpha 300R confocal Raman microscope equipped with 100× air objective and 600 grooves/mm grating. Surface scan of (14 × 18) μm^2 and depth scan (5 μm) were done using 532 nm laser source and a back illuminated CCD detector. Surface area was determined using Quanta chrome Nova 1200e surface area analyzer using the Brunauer−Emmett−Teller (BET) method. The material was heated at 150 °C under helium flow for 15 min before any characterization technique.

2.4. CO_2 Adsorption/Desorption Studies. *Thermogravimetric Method.* CO_2 adsorption/desorption studies were carried out using a PerkinElmer Pyris 1 thermogravimetric analyzer with purge gas switching accessory with about 10 mg of sample in a platinum pan. Pure CO_2 (99.99%), CO_2-N_2 mixture (10:90), and ambient air (400 ppm at RH 60%) were used for CO_2 adsorption studies. The CO_2 adsorption capacity was estimated from the weight gain of the sorbent after exposure to CO_2 using a gas flow rate of 100 mL/min. Desorption studies were done at 80 °C under He flow (70 mL/min). The material was heated at 150 °C under He flow (30 mL/min) for 15 min before any CO_2 adsorption study.

The cyclic regeneration studies of the sorbent materials were also done with TG analyzer using 100% CO_2 and ambient air under the same conditions used in adsorption/desorption as detailed above.

Packed Column Adsorption. MAHSM (12.0 g) was packed in a glass tube (20 cm × 3 cm). The material was heated at 150 °C under N_2 flow (100 mL/min) for 15 min. After cooling, ambient air (RH 85%, 28 °C) containing 350 ppm of CO_2 was passed through the sorbent at a flow rate of 500 mL/min. The input and output CO_2 concentrations were measured using IR detector.

3. RESULTS AND DISCUSSION

3.1. Synthesis of Sorbent and Characterization. The sorbent was developed on the basis of the hydrolytic co-condensation reaction of amino propyl and vinyl functionalized triethoxysilanes.[51] Aminosilane acts as internal catalyst for the hydrolysis and condensation reactions in the silane mixture. Different types of silsesquioxanes, viz., cage, ladder, and network, were reported to be formed by hydrolytic co-condensation reactions.[50−54] A general scheme for the reaction is shown in Scheme S1. The optimizations of the mole ratio of silanes/ethanol/water, stirring time, aging period, and final molar concentration of silanes/ethanol/water for the preparation of hybrid silica materials were done on the basis of the CO_2 adsorption/desorption performance and thermal stability of the product material. Aminosilane (AS) and vinylsilane (VS) at 1:1 molar ratio was optimized for an aging period of 5 days (Tables S1 and S2).

In the synthesis of the material, after aging the silane mixture it was diluted with absolute alcohol before spraying down to

DOI: 10.1021/acsami.5b04674
ACS Appl. Mater. Interfaces 2015, 7, 17969−17976

make the final product (MAHSM). The morphology of the material changed as revealed from the SEM images as shown in Figure 1. The "bottleneck" regions as visible in Figure 1a were

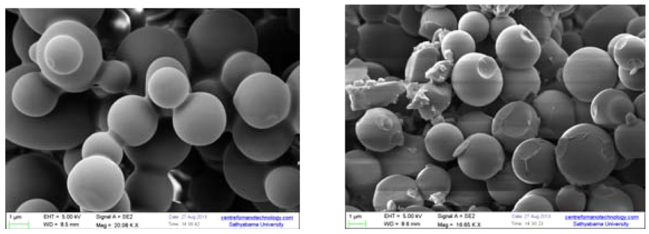

(a) (b)

Figure 1. Change in morphology of MAHSM (a) material as such prepared from aged siloxane solution and (b) material prepared after dilution of aged siloxane solution.

broken, and discrete microspheres (1−3.5 μm) were formed as in Figure 1b when prepared after dilution of aged siloxane solution. An interesting feature observed was that CO_2 capture capacity increased when the material was prepared after dilution (Table S1). This can be explained as possibly due to the more "exposed reaction sites" (amino groups) made available for CO_2 by breaking the agglomeration and forming independent microspheres upon dilution.

FT-IR spectrum (Figure S1) of MAHSM features Si−O−Si_{str} at 1138 and 1039 cm^{-1}. The peak 1138 cm^{-1} is characteristic of caged (T_8) silsesquioxane,[55−57] and the one at 1039 cm^{-1} may be attributed to ladder/network polysilsesquioxane.[57−59] Also, the "peak shape" in 1030−1130 cm^{-1} range is generally being considered as the characteristic of structured silsesquioxane.[60] Other spectral bands are for vinyl (3060, 1410 cm^{-1}), amino propyl (3367, 3291, 2933, and 1602 cm^{-1}), and Si−OH (964 cm^{-1}).

Solid-state ^{13}C and ^{29}Si CP-MAS NMR data (Figure S2) were used to characterize the chemical structure of the material. ^{13}C CP-MAS NMR spectra showed resonance peaks at 131.9 and 135.2 ppm corresponding to vinyl groups. Peaks at 11.3, 25.2, and 44.4 ppm represent the $-(CH_2)_3NH_2$ moiety. ^{29}Si CP-MAS NMR spectra showed peaks at −80.1 and −66.8 ppm corresponding to fully condensed T^3 vinyl and amino propyl species, respectively. A small shoulder peak at −57.6 ppm is due to T^2 species resulting from incomplete condensation. NMR data suggest relatively fully condensed polysilsesquioxane formation in MAHSM.

Raman spectrum (Figure S3) showed a peak at 483 cm^{-1} corresponding to Si−O−Si_{str} (sym) of cross-linked network siloxane.[61] Other peaks of interest are 1600 cm^{-1} ($-NH_2$ sci), 3303 cm^{-1} ($-NH_2$ sym), 3370 cm^{-1} ($-NH_2$ asym), and 1408 cm^{-1} (vinyl). A Raman spectral image as in Figure 2a was generated by scanning over an area of (14 × 18) μm^2 MAHSM aggregate and integrating over characteristic amine and vinyl vibrations, and the Raman spectra remained the same throughout the area of scan. In the image, the black portion corresponds to substrate on which the sample is placed, and the red/yellow part corresponds to the sample. It can be seen that the Raman image is similar to the SEM image of MAHSM, showing hybrid silica microspheres. The line scan (x−y scan) and depth scan (z) using the wavelengths 1600 cm^{-1} ($-NH_2$ sci), 3303 cm^{-1} ($-NH_2$ sym), and 1408 cm^{-1} (vinyl) generated the same cross-sectional profile as in Figure 2b indicating vinyl and amine moieties are homogeneously distributed throughout the material.

The wave-like pattern in the cross-sectional profile (through the blue line in the image) is due to the spherical nature of the particle which causes a change in focus during scan, and the distances between consecutive troughs give the diameter of the sphere-like particles.

The C/N ratio of MAHSM was calculated from elemental analysis (C 26.1%, H 4.8%, N 6.3%). Eight different batches of MAHSM were analyzed, and these studies found that the C/N mole ratio falls at 4.9 ± 0.3 which is close to the theoretical value (5.0). This further confirms the homogeneity of sorbent with respect to amine and vinyl distribution as inferred from Raman imaging. Low BET surface area (0.9 m^2/g) and SEM analysis point out that hybrid silica sorbent synthesized through this method is not mesoporous.

The XRD pattern shows broad reflections at 2θ values of 8.8° and 22° (Figure S4). Generally, peaks at ∼8° and ∼20° are regarded as characteristic crystalline reflections from caged silsesquioxanes, and in particular, the peak at 8° is attributed to the d-spacing caused by the size of the polyhedral oligomeric silsesquioxane (POSS) molecule. Pavithran et al.[51] assigned the peak at 8° to POSS and the one at 20° to hexagonal or rhombohedral packing of POSS cages in siloxane polymeric halo. In the case of MAHSM, the XRD pattern obtained was of diffused type conforming more toward amorphous nature. The 2θ and d values (8.8°, 10.1 Å) are close to the values reported

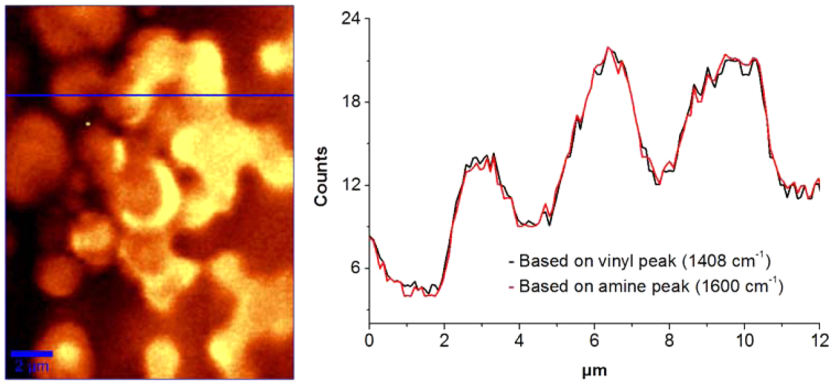

(a) (b)

Figure 2. (a) Raman image and (b) cross-sectional profile across the line in part a.

DOI: 10.1021/acsami.5b04674
ACS Appl. Mater. Interfaces 2015, 7, 17969−17976

for POSS−polymer nanocomposites.[62−64] A similar XRD pattern and *d* values were reported for ladder or network polysilsesquioxane also.[53,54]

Even though the IR spectrum and XRD pattern of hybrid silica indicate the formation of POSS cage, the IR peak at 1030 cm^{-1} corresponds to the formation of ladder/network silsesquioxane, and Raman peak at 483 cm^{-1} indicates cross-linked network silsesquioxane. The hybrid silica material is insoluble in all common organic solvents, suggesting the formation of cross-linked network silsesquioxanes. Thus, the possibility of the existence of cage, ladder, and network silsesquioxane together in the material cannot be ruled out. As the existence of ladder silsesquioxanes in our system is not proven unambiguously, on the basis of the available information, the hybrid silica materials are better viewed as crystalline aggregates of POSS cages distributed in cross-linked network silsesquioxane polymer. Lei Zheng et al. proposed an ordered arrangement of cubic silsesquioxane nanoparticles in the polyethylene-*co*-POSS[62] system and, later, for the polybutadiene-POSS nanocomposite system.[64] In the present case, the self-aggregation of POSS nanoparticles can happen in network silsesquioxane polymer and will be controlled by vinyl and amino groups. The hydrophobic vinyl groups help in deciding the orientation of amino groups and lead to a "relatively structured" polysilsesquioxane hybrid silica material. The layered structure of MAHSM is evident in the HR-TEM image (Figure 3).

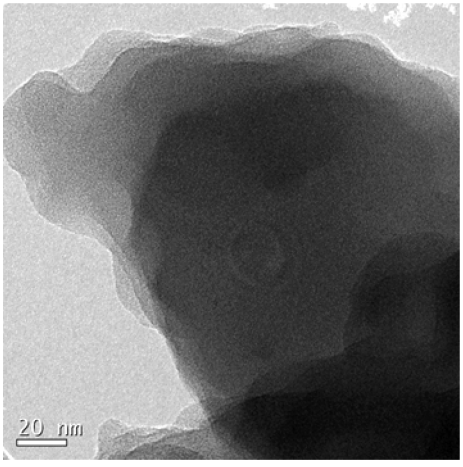

Figure 3. HR-TEM image of MAHSM.

The thermal stability of MAHSM is confirmed by thermogravimetric analysis (Figure S5) which shows that the sorbents are stable up to 300 °C under inert atmosphere. The organic matter decomposes above 300 °C resulting in the formation of stable residue at 800 °C. The decomposition temperature for 5% weight loss, $T_{d\ (5\%)}$, obtained for MAHSM was 458 °C which shows the quality of the material for using it as a thermally regenerable sorbent.

3.2. CO_2 Adsorption Characteristics. The hybrid silica sorbent, MAHSM, was analyzed for CO_2 adsorption capacity using thermogravimetric analyzer under different partial pressures of CO_2. MAHSM showed a maximum CO_2 adsorption of 2.28 mmol/g in 100% CO_2 and 1.92 mmol/g in 10% CO_2, at a flow rate of 100 mL/min at 30 °C. The experimental adsorption capacity of MAHSM in 100% CO_2 is closely matching with the theoretical value of 2.25 mmol/g (assuming 100% carbamate conversion for an amine content of 4.5 mmol N/g of MAHSM). The heat of absorption value of −85 ± 5 kJ/mol CO_2 obtained from isothermal differential scanning calorimetry (Figure S6) for 3 different measurements indicates that the process involving adsorption of CO_2 to MAHSM is a chemical interaction.

The sorbent was also evaluated for the adsorption of CO_2 from ambient air (containing 400 ppm of CO_2, 60% RH) at 30 °C with a flow rate of 100 mL/min in 24 h, and a CO_2 adsorption capacity of 1.68 mmol/g was obtained. A comparison of CO_2 adsorption by MAHSM under different CO_2 partial pressures is shown in Figure 4.

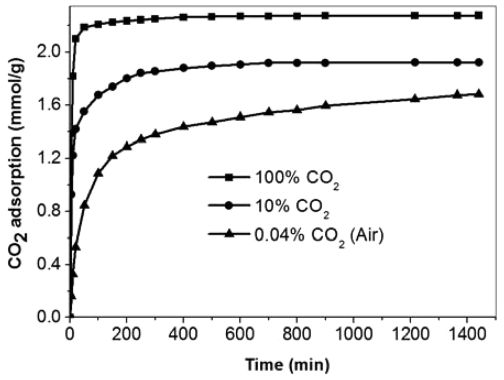

Figure 4. Comparison of CO_2 adsorption of MAHSM at different CO_2 concentration.

The CO_2 adsorption studies using 100% CO_2, 10% CO_2, and air (0.04% CO_2) suggest that the adsorption capacity of the hybrid silica sorbent is not depreciated significantly even with ultradilution in CO_2 concentration. When the CO_2 concentration was reduced by a factor of 250 (from 10% to 400 ppm), the adsorption capacity of MAHSM decreased only by a factor of 1.1 showing the capability of the sorbent to capture CO_2 from extreme dilutions. It may be noted that for HAS sorbents this factor was reported as 2.2.[44] The TG-MS analysis of the sorbent material after CO_2 adsorption from ambient air (Figure S7) shows a peak corresponding to CO_2 (*m*/*z* 44) alone. Thus, it is confirmed that the total weight gain after adsorption from air is entirely due to CO_2. Absence of a moisture peak in TG-MS points toward the hydrophobic nature of the sorbent.

Further, it was observed that CO_2 adsorption from ambient air decreases with increase of temperature (Figure S8). The CO_2 adsorption capacity decreased from 1.68 mmol/g at 30 °C to 1.08 mmol/g at 50 °C. The adsorption half time (time for reaching half of the adsorption capacity at saturation) and average rate of adsorption to reach the half-maximum were used for comparison among reported sorbents by many researchers. Choi et al.[36,44] compared the adsorption half time (T_{half}), and Gebald et al.[65] additionally used average rate of CO_2 adsorption to reach T_{half} for comparison among different adsorbents. MAHSM showed an adsorption half time of 50 min reached at the rate of 17.9 μmols/g/min during CO_2 capture from air under the given conditions of the experiment. An amine efficiency (37.3%) of MAHSM (1.68 mmol CO_2 from air by 4.5 mmol N) in air capture is far better than many of the reported materials. Table S3 shows a comparison among similar regenerable sorbents reported for direct CO_2 capture from ambient air.

DOI: 10.1021/acsami.5b04674
ACS Appl. Mater. Interfaces 2015, 7, 17969−17976

Lab level studies were conducted to evaluate the CO_2 adsorption behavior from ambient air (RH 85%, 28 °C containing 350 ppm of CO_2), with higher sample loading, using a separate packed column setup. Figure 5 shows the result obtained for CO_2 adsorption from air using a packed column experiment.

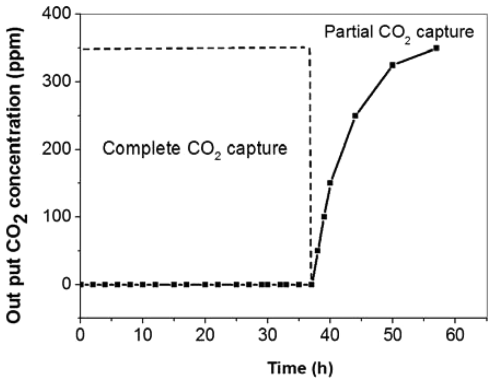

Figure 5. Adsorption of CO_2 from air using packed column.

The first part represents the complete adsorption of CO_2 from air giving zero output CO_2 concentration, which lasted for 37 h. After this period, the material started to get saturated slowly and gave output CO_2 concentration ranging from 50 to 200 ppm, which continued until 56 h, and got fully saturated. The total CO_2 adsorption from ambient air was 19.1 mmol of CO_2 by 12.0 g of sorbent corresponding to 1.59 mmol CO_2/g. Desorption was done at 80 °C under N_2 flow (100 mL/min) for 30 min. This experiment, given the worst environment for capturing CO_2 competing with moisture and other gases in air, proves the efficiency of MAHSM as a real CO_2 capturing material.

The quick adsorption of CO_2 from extreme dilution as that from atmospheric air is attributed to the easy accessibility of primary amino groups, a direct output from the layered arrangement of polysilsesquioxanes. The layered structure further helps in the easy regeneration of CO_2. Also, hydrophobic nature of the material kept away moisture when compared to sorbent systems based on mesoporous materials.

3.3. CO_2 Desorption Characteristics. Desorption starts at a lower temperature, 60 °C, and >50% desorption is completed within 5 min, but complete desorption happens at 80 °C in 10 min (Figure S9). Figure S10 shows the IR spectra of MAHSM after CO_2 adsorption (a) and desorption (b). The peaks at 1642 (NH_3^+ def), 1568 (asym COO^-), 1489 (sym NH_3^+ def), and 1340 cm^{-1} (sym COO^-) are indicative of CO_2 adsorption/desorption.[66−68] It may be noted that all these peaks are corresponding to the weak ionic carbamate species formed with the amino groups, and there are no bound carbamates as evidenced by the absence of peaks at 1710−1715 cm^{-1} (C═O str) and 1510 cm^{-1} (NH def + C—N str). The bound carbamate moiety (1715−1710 cm^{-1}) was assigned as silyl propyl carbamate (Figure S11) by Zoltan Bacsik et al.[68] in agreement with the findings of Danon et al.[66]

Even though silanol groups are present, the hydrophobic vinyl groups decide the orientation of the POSS aggregation and minimize silanol−carbamic acid interaction, thereby preventing silyl propyl carbamate formation. This again emphasizes the stable orientation of POSS and network silsesquioxane in the sorbent system as discussed. The absence of bound carbamate (silyl propyl carbamate) in the present sorbent is beneficial in the easy regeneration after CO_2 adsorption and will ultimately be helpful in giving high cyclic utility and life for the sorbent.

3.4. Cyclic Studies. In 100% CO_2, adsorption is very fast, and >80% of the reaction is completed in less than 15 min. Hence, the adsorption/desorption half cycles were fixed at 15 min. Up to 100 cycles of regeneration (Figure 6) were successfully demonstrated using MAHSM without any loss in efficiency.

The cyclic ability of MAHSM for the removal of CO_2 from ambient air (400 ppm of CO_2, 30 °C, RH 60%) was also demonstrated. As CO_2 adsorption capacity of MAHSM reaches >1.0 mmol/g in 100 min, adsorption was performed for 100 min, and desorption was done for 15 min. Figure 7 shows 50 consecutive regeneration cycles performed in ambient air with MAHSM.

Urea formation is reported as a side reaction that could limit the cyclic utility of amine sorbents. Sayari et al.[69] studied the CO_2 induced degradation of grafted amine sorbents and reported that, after 30 thermal cycles at 50/130 °C of monoamine-based sorbent, the carbamate carbonyl peak (^{13}C CP-MAS NMR) at 164.5 ppm shifted to 159.6 ppm suggesting the formation of urea which resulted in 65% CO_2 uptake loss. In the case of MAHSM, 50 cycles were performed at 30 °C in ambient air followed by desorption at 80 °C under He flow. The sorbent, after the 1st and 50th adsorption cycles, was analyzed by ^{13}C CP-MAS NMR, and the peak appeared at 164.5 ppm in both cases. To check whether the lack of urea formation is due to residual moisture resulting from low regeneration temperature, 40 regeneration cycles of adsorption at 30 °C (100% CO_2,100 mL/min, 15 min) and desorption at 120 °C (He flow, 70 mL/min, 15 min) were done. As in the

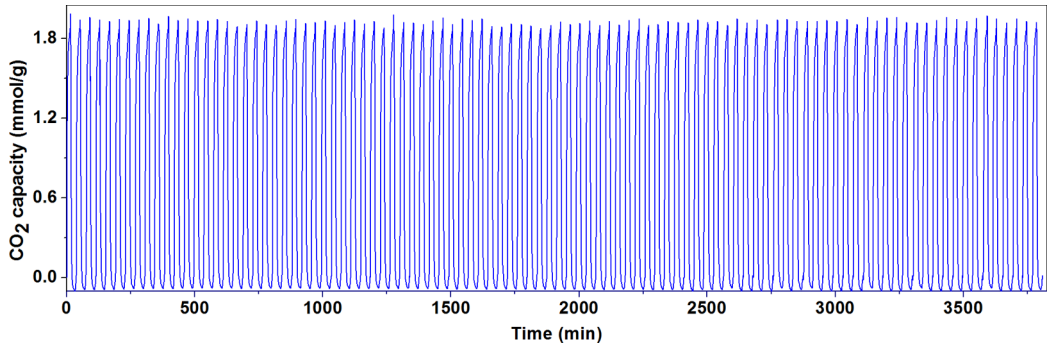

Figure 6. Cyclic capacity of MAHSM (100 cycles) in pure CO_2.

DOI: 10.1021/acsami.5b04674
ACS Appl. Mater. Interfaces 2015, 7, 17969−17976

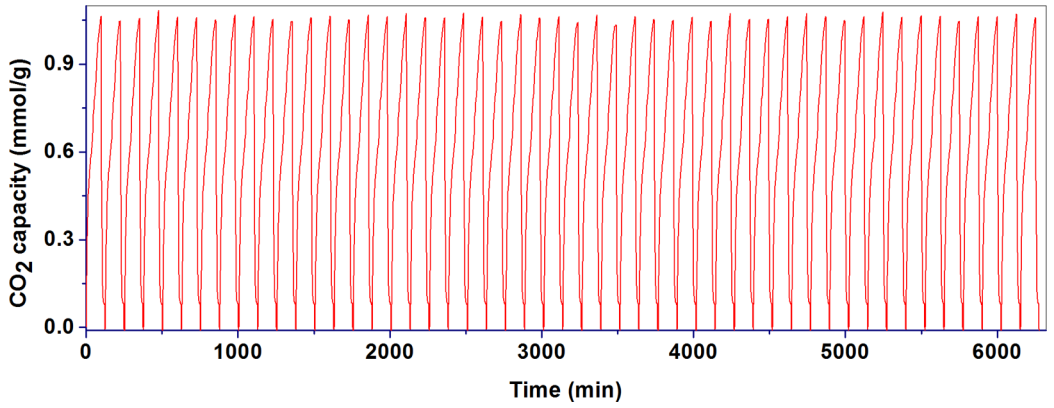

Figure 7. Cyclic capacity of MAHSM (50 cycles) in ambient air.

case of cycling from air, no shift in carbamate peak position (Figure S12) or loss in CO_2 adsorption efficiency was observed.

4. CONCLUSIONS

Functionalized polysilsesquioxane-based structured hybrid silica materials are developed as regenerable sorbents for the removal of carbon dioxide from atmospheric air. The developed material (MAHSM) captured a maximum of 1.68 mmol/g CO_2 from ambient air in 24 h, with an adsorption half time of 50 min reached at the rate of 17.9 μmols/g/min, indicating a suitable candidate for air capture applications. CO_2 adsorption capacities of 2.28 mmol/g in pure CO_2 and 1.92 mmol/g in 10% CO_2 were also demonstrated. Easy and energy efficient production route, low temperature regeneration, and high CO_2 cyclic capability make these materials "interesting" candidates for the CO_2 removal process. This material can also find application in closed habitats like submarines, space craft crew cabins, or any other systems requiring CO_2-free air. Apart from the inherent CO_2 selectivity provided by the amino groups, the hydrophobic nature of the material prevents moisture uptake from air and hence can be further explored as hydrophobic coating materials capturing CO_2 directly from the atmosphere.

■ ASSOCIATED CONTENT

Supporting Information

Scheme S1, Figures S1−S12, and Tables S1−S3. The Supporting Information is available free of charge on the ACS Publications website at DOI: 10.1021/acsami.5b04674.

(PDF)

■ AUTHOR INFORMATION

Corresponding Author

*Fax: 914712564096. Phone: 914712564299. E-mail: abhilashkadisser@gmail.com.

Notes

The authors declare no competing financial interest.

■ ACKNOWLEDGMENTS

We express our sincere gratitude to Director, VSSC, and Deputy Director, VSSC (PCM), for permission to publish this work. The support and guidance given by Dr. S. Packirisamy and Dr. C. P. Reghunathan Nair are gratefully acknowledged. We are thankful to Dr. K. P. Vijayalakshmi, S. Bhuvaneswari, N. Supriya, T. Jayalatha, R. Radhika, and Nisha Balachandran for analytical support.

■ ABBREVIATIONS

AS = 3-amino propyl triethoxysilane
VS = vinyl triethoxysilane
MAHSM = monoamine-based hybrid silica material
TRI-PE-MCM-41 = triamine-grafted pore expanded mesoporous silica
HAS = hyperbranched amino silica
POSS = polyhedral oligomeric silsesquioxane
AEAPDMS-NFC-FD = aminosilane modified nanofibrillated cellulose aerogel
MOF = metal organic framework
CP-MAS = cross-polarization-magic angle spinning
NMR = nuclear magnetic resonance spectroscopy
FTIR = Fourier transform infrared spectroscopy
FESEM = field emission scanning electron microscopy
HRTEM = high resolution transmission electron microscopy
TGA = thermogravimetric analyzer
GC−MS = gas chromatography−mass spectrometry

■ REFERENCES

(1) Keith, D. W. Why Capture CO_2 from the Atmosphere? *Science* **2009**, *325*, 1654−1655.
(2) Lackner, K. S. Capture of Carbon dioxide from Ambient Air. *Eur. Phys. J.: Spec. Top.* **2009**, *176*, 93−106.
(3) Goeppert, A.; Czaun, M.; Surya Prakash, G. K.; Olah, G. A. Air as the Renewable Carbon Source of the Future: An overview of CO_2 Capture from the Atmosphere Energy. *Energy Environ. Sci.* **2012**, *5*, 7833−7853.
(4) Nikulshina, V.; Hirsch, D.; Steinfeld, A. CO_2 capture from Atmospheric air via Consecutive CaO-Carbonation and $CaCO_3$-Calcination cycles in a Fluidized-bed Solar Reactor. *Chem. Eng. J.* **2009**, *146*, 244−248.
(5) Nikulshina, V.; Gebald, C.; Mazzotti, M.; Steinfeld, A. CO_2 Capture from Air and Co-production of H_2 via the $Ca(OH)_2$−$CaCO_3$ Cycle Using Concentrated Solar Power-Thermodynamic Analysis. *Energy* **2006**, *31*, 1715−1725.
(6) Mahmoudkhani, M.; Keith, D. W. Low-energy Sodium hydroxide Recovery for CO_2 Capture from Atmospheric Air-Thermodynamic Analysis. *Int. J. Greenhouse Gas Control* **2009**, *3*, 376−384.
(7) D'Alessandro, D. M.; Smit, B.; Long, J. R. Carbon dioxide Capture: Prospects for New Materials. *Angew. Chem., Int. Ed.* **2010**, *49*, 6058−6082.
(8) Stuckert, N. R.; Yang, R. T. CO_2 capture from the Atmosphere and Simultaneous Concentration using Zeolites and Amine-grafted SBA-15. *Environ. Sci. Technol.* **2011**, *45*, 10257−64.
(9) Zhang, C.; Song, W.; Sun, G.; Xie, L.; Wang, J.; Li, K.; Sun, C.; Liu, H.; Snape, C. E.; Drage, T. CO_2 capture with Activated Carbon Grafted by Nitrogenous Functional Groups. *Energy Fuels* **2013**, *27*, 4818−4823.

DOI: 10.1021/acsami.5b04674
ACS Appl. Mater. Interfaces 2015, 7, 17969−17976

(10) Wickramaratne, N. P.; Jaroniec, M. Activated Carbon Spheres for CO_2 Adsorption. *ACS Appl. Mater. Interfaces* **2013**, *5*, 1849−1855.
(11) Sumida, K.; Rogow, D. L.; Mason, J. A.; McDonald, T. M.; Bloch, E. D.; Herm, Z. R.; Bae, T. H.; Long, J. R. Carbon dioxide Capture in Metal-Organic Frameworks. *Chem. Rev.* **2012**, *112*, 724−781.
(12) Hayashi, H.; Cote, A. P.; Furukawa, H.; O'Keeffe, M.; Yaghi, O. M. Zeolite A imidazolate frameworks. *Nat. Mater.* **2007**, *6*, 501−506.
(13) McDonald, T. M.; Lee, W. R.; Mason, J. A.; Wiers, B. M.; Hong, C. S.; Long, J. R. Capture of Carbon dioxide from Air and Flue Gas in the Alkylamine-Appended Metal−Organic Framework mmen-Mg_2(dobpdc). *J. Am. Chem. Soc.* **2012**, *134*, 7056−7065.
(14) Choi, S.; Watanabe, T.; Bae, T. H.; Sholl, D. S.; Jones, C. W. Modification of the Mg/DOBDC MOF with Amines to Enhance CO_2 Adsorption from Ultra dilute Gases. *J. Phys. Chem. Lett.* **2012**, *3*, 1136−1141.
(15) Lee, W. R.; Hwang, S. Y.; Ryu, D. W.; Lim, K. S.; Han, S. S.; Moon, D.; Choi, J.; Hong, C. S. Diamine-Functionalized Metal−Organic Framework: Exceptionally high CO_2 capacities from Ambient Air and Flue gas, Ultrafast CO_2 uptake rate, and Adsorption Mechanism Energy. *Energy Environ. Sci.* **2014**, *7*, 744−751.
(16) Nugent, P.; Belmabkhout, Y.; Burd, S. D.; Cairns, A. J.; Luebke, R.; Forrest, K.; Pham, T.; Ma, S.; Space, B.; Wojtas, L.; Eddaoudi, M.; Zaworotko, M. J. Porous Materials with Optimal Adsorption Thermodynamics and Kinetics for CO_2 Separation. *Nature* **2013**, *495*, 80−84.
(17) Vaidhyanathan, R.; Iremonger, S. S.; Dawsona, K. W.; Shimizu, G. K. H. An amine-functionalized Metal Organic Framework for Preferential CO_2 Adsorption at Low pressures. *Chem. Commun.* **2009**, 5230−5232.
(18) Shekhah, O.; Belmabkhout, Y.; Chen, Z.; Guillerm, V.; Cairns, A.; Adil, K.; Eddaoudi, M. Made-to-order Metal-Organic Frameworks for Trace Carbon dioxide Removal and Air Capture. *Nat. Commun.* **2014**, *5*, 5.
(19) Zhang, M.; Perry, M.; Park, J.; Zhou, H. C. Stable Benzimidazole-Incorporated Porous Polymer Network for Carbon Capture with High efficiency and Low cost. *Polymer* **2014**, *55*, 335−339.
(20) Lu, W.; Sculley, J. P.; Yuan, D.; Krishna, R.; Wei, Z.; Zhou, H. C. Polyamine-Tethered Porous Polymer Networks for Carbon dioxide Capture from Flue Gas. *Angew. Chem., Int. Ed.* **2012**, *51*, 7480−7484.
(21) Lu, W.; Sculley, J. P.; Yuan, D.; Krishna, R.; Zhou, H. C. Carbon dioxide Capture from Air Using Amine-Grafted Porous Polymer Networks. *J. Phys. Chem. C* **2013**, *117*, 4057−4061.
(22) Dutcher, B.; Fan, M.; Russell, A. G. Amine-Based CO_2 Capture Technology Development from the Beginning of 2013-A Review. *ACS Appl. Mater. Interfaces* **2015**, *7*, 2137−2148.
(23) Kong, Y.; Shen, X.; Cui, S.; Fan, M. Facile Synthesis of an Amine Hybrid Aerogel with High Adsorption Efficiency and Regenerability for Air Capture via a Solvothermal-Assisted Sol-Gel Process and Supercritical Drying. *Green Chem.* **2015**, *17*, 3436−3445.
(24) Satyapal, S.; Filburn, T.; Trela, J.; Strange, J. Performance and Properties of a Solid Amine Sorbent for Carbon dioxide Removal in Space Life Support Applications. *Energy Fuels* **2001**, *15*, 250−255.
(25) Hwang, C. C.; Jin, Z.; Lu, W.; Sun, Z.; Alemany, L. B.; Lomeda, J. R.; Tour, J. M. In situ Synthesis of Polymer-Modified Mesoporous Carbon CMK-3 Composites for CO_2 Sequestration. *ACS Appl. Mater. Interfaces* **2011**, *3*, 4782−4786.
(26) Kenarsari, S. D.; Yang, D.; Jiang, S.; Zhang, S.; Wang, J.; Russell, A. G.; Wei, Q.; Fan, M. Review of Recent Advances in Carbon dioxide Separation and Capture. *RSC Adv.* **2013**, *3*, 22739−22773.
(27) Jones, C. W. CO_2 Capture from Dilute Gases as a Component of Modern Global Carbon Management. *Annu. Rev. Chem. Biomol. Eng.* **2011**, *2*, 31−52.
(28) Zhao, A.; Samanta, A.; Sarkar, P.; Gupta, R. Carbon dioxide Adsorption on Amine-Impregnated Mesoporous SBA-15 Sorbents: Experimental and Kinetics Study. *Ind. Eng. Chem. Res.* **2013**, *52*, 6480−6491.
(29) Qi, G.; Wang, Y.; Estevez, L.; Duan, X.; Anako, N.; Park, A. H. A; Li, W.; Jones, C. W.; Giannelis, E. P. High Efficiency Nanocomposite Sorbents for CO_2 Capture based on Amine-Functionalized Mesoporous Capsules. *Energy Environ. Sci.* **2011**, *4*, 444−452.
(30) Goeppert, A.; Czaun, M.; May, R. B.; Surya Prakash, G. K.; Olah, G. A.; Narayanan, S. R. Carbon dioxide Capture from the Air Using a Polyamine Based Regenerable Solid Adsorbent. *J. Am. Chem. Soc.* **2011**, *133*, 20164−20167.
(31) Knowles, G. P.; Webley, P. A.; Liang, Z.; Chaffee, A. L. Silica/polyethyleneimine Composite Adsorbent S-PEI for CO_2 Capture by Vacuum Swing Adsorption (VSA), in Recent Advances in Post-Combustion CO_2 Capture Chemistry. *ACS Symp. Ser.* **2012**, *1097*, 177−205.
(32) Sculley, J. P.; Zhou, H. C. Enhancing Amine-Supported Materials for Ambient Air Capture. *Angew. Chem., Int. Ed.* **2012**, *51*, 12660−12661.
(33) Xu, X.; Song, C.; Andresen, J. M.; Miller, B. G.; Scaroni, A. W. Novel Polyethylenimine-Modified Mesoporous Molecular sieve of MCM-41 type as High-Capacity Adsorbent for CO_2 Capture Energy. *Energy Fuels* **2002**, *16*, 1463−1469.
(34) Bollini, P.; Didas, S. A.; Jones, C. W. Amine-oxide Hybrid Materials for Acid Gas Separations. *J. Mater. Chem.* **2011**, *21*, 15100−15120.
(35) Tanthana, J.; Chuang, S. S. C. In situ Infrared Study of the Role of PEG in Stabilizing Silica-Supported Amines for CO_2 Capture. *ChemSusChem* **2010**, *3*, 957−964.
(36) Choi, S.; Gray, M. L.; Jones, C. W. Amine-tethered Solid Adsorbents Coupling High Adsorption Capacity and Regenerability for CO_2 Capture from Ambient Air. *ChemSusChem* **2011**, *4*, 628−635.
(37) Gunathilake, C.; Jaroniec, M. Mesoporous Organosilica with Amidoxime Groups for CO_2 Sorption. *ACS Appl. Mater. Interfaces* **2014**, *6*, 13069−13078.
(38) Prempeh, G. O.; Lehmler, H. J.; Rankin, E. S.; Knutson, B. L. Direct Synthesis and Accessibility of Amine-Functionalized Mesoporous Silica Template Using Fluorinated Surfactants. *Ind. Eng. Chem. Res.* **2011**, *50*, 5510−5522.
(39) Zelenák, V.; Badanicová, M.; Halamová, D.; Cejka, J.; Zukal, A.; Murafa, N.; Goerigk, G. Amine-Modified ordered Mesoporous Silica: Effect of Pore size on Carbon dioxide Capture. *Chem. Eng. J.* **2008**, *144*, 336−342.
(40) Loganathan, S.; Tikmani, M.; Ghoshal, A. K. A Novel Pore Expanded MCM-41 for CO_2 Capture: Synthesis and Characterization. *Langmuir* **2013**, *29*, 3491−3499.
(41) Belmabkhout, Y.; Guerrero, R. S.; Sayari, A. Amine-bearing Mesoporous Silica for CO_2 removal from dry and humid air. *Chem. Eng. Sci.* **2010**, *65*, 3695−3698.
(42) Belmabkhout, Y.; Guerrero, R. S.; Sayari, A. Adsorption of CO_2-Containing Gas Mixtures over Amine-Bearing Pore-Expanded MCM-41 Silica: Application for Gas Purification. *Ind. Eng. Chem. Res.* **2010**, *49*, 359−365.
(43) Sayari, A.; Belmabkhout, Y. Stabilization of Amine-containing CO_2 Adsorbents: Dramatic Effect of Water vapor. *J. Am. Chem. Soc.* **2010**, *132*, 6312−6314.
(44) Choi, S.; Drese, J. H.; Eisenberger, P. M.; Jones, C. W. Application of Amine-Tethered Solid Sorbents for Direct CO_2 Capture from the Ambient Air. *Environ. Sci. Technol.* **2011**, *45*, 2420−2427.
(45) Kim, S. N.; Son, W. J.; Choi, J. S.; Ahn, W. S. CO_2 Adsorption using Amine-Functionalized Mesoporous Silica Prepared via Anionic Surfactant-Mediated Synthesis Microporous. *Microporous Mesoporous Mater.* **2008**, *115*, 497−503.
(46) Hao, S.; Chang, H.; Xiao, Q.; Zhong, Y.; Zhu, W. One-pot Synthesis and CO_2 Adsorption Properties of Ordered Mesoporous SBA-15 Materials Functionalized with APTMS. *J. Phys. Chem. C* **2011**, *115*, 12873−12882.
(47) Klinthong, W.; Chao, K. J.; Tan, C. S. CO_2 Capture by As-Synthesized Amine-Functionalized MCM-41 Prepared through Direct

DOI: 10.1021/acsami.5b04674
ACS Appl. Mater. Interfaces 2015, 7, 17969−17976

Synthesis under Basic Condition. *Ind. Eng. Chem. Res.* **2013**, *52*, 9834−9842.
(48) Qi, G.; Fu, L.; Duan, X.; Choi, B. H.; Abraham, M.; Giannelis, E. P. Mesoporous Amine-Bridged Polysilsesquioxane for CO_2 capture Greenhouse Gases. *Greenhouse Gases: Sci. Technol.* **2011**, *1*, 278−284.
(49) Shanmugam, N.; Lee, K. T.; Cheng, W. Y.; Lu, S. Y. Organic−Inorganic Hybrid Polyaspartimide involving Polyhedral Oligomeric Silsesquioxane via Michael addition for CO_2 Capture. *J. Polym. Sci., Part A: Polym. Chem.* **2012**, *50*, 2521−2526.
(50) Voronkov, M. G.; Larent' yev, V. I. Polyhedral Oligosilsesquioxanes and their Homo Derivatives. *Top. Curr. Chem.* **1982**, *102*, 199−236.
(51) Nair, B. P.; Pavithran, C. Bifunctionalized Hybrid Silica Spheres by Hydrolytic Co-condensation of 3-Aminopropyltriethoxysilane and Vinyltriethoxysilane. *Langmuir* **2010**, *26*, 730−735.
(52) Sankaraiah, S.; Lee, J. M.; Kim, J. H.; Choi, S. W. Preparation and Characterization of Surface-Functionalized Polysilsesquioxane Hard Spheres in Aqueous Medium. *Macromolecules* **2008**, *41*, 6195−6204.
(53) Liu, S.; Lang, X.; Ye, H.; Zhang, S.; Zhao, J. Preparation and Characterization of Copolymerized Aminopropyl/Phenyl Silsesquioxane Microparticles. *Eur. Polym. J.* **2005**, *41*, 996−1001.
(54) Dong, F.; Guo, W.; Chu, S. W.; Ha, C. S. Novel Fluorinated Polysilsesquioxane Hollow spheres: Synthesis and Application in Drug release. *Chem. Commun.* **2010**, *46*, 7498−7500.
(55) Chen, C.; Chen, M.; Huang, S. Synthesis and Characterization of Monofunctionalized Polyhedral Oligomeric Silsesquioxanes by Cohydrolytic and Cocondensation of Propyltrimethoxysilane and Vinyltrimethoxysilane. *J. Macromol. Sci., Part A: Pure Appl.Chem.* **2011**, *48*, 478−481.
(56) Baney, R. H.; Itoh, M.; Sakakibara, A.; Suzuki, T. Silsesquioxanes. *Chem. Rev.* **1995**, *95*, 1409−1430.
(57) Park, E. S.; Ro, H. W.; Nguyen, C. V.; Jaffe, R. L.; Yoon, D. Y. Infrared Spectroscopy Study of Microstructures of Poly-(silsesquioxane)s. *Chem. Mater.* **2008**, *20*, 1548−1554.
(58) Chomel, A. D.; Dempsey, P.; Latournerie, J.; Bahloul, D. H.; Jayasooriya, U. A. *Gel to Glass transformation of Methyltriethoxysilane: A Silicon Oxycarbide Glass Precursor Investigated using Vibrational Spectroscopy*. *Chem. Mater.* **2005**, *17*, 4468−4473.
(59) Unno, M.; Suto, A.; Matsumoto, T. Laddersiloxanes — Silsesquioxanes with Defined Ladder structure Russ. *Russ. Chem. Rev.* **2013**, *82*, 289−302.
(60) Smith, A. L. *Analysis of Silicones*; John Wiley & Sons: New York, 1974; Chapter 10, pp 275−279.
(61) Caster, A. G.; Kowarik, S.; Schwartzberg, A. M.; Nicolet, O.; Lim, S. H.; Leone, S. R. Observing Hydrogen Silsesquioxane Cross-linking with Broadband CARS. *J. Raman Spectrosc.* **2009**, *40*, 770−774.
(62) Zheng, L.; Waddon, A. J.; Farris, R. J.; Coughlin, E. B. X-ray Characterizations of Polyethylene Polyhedral Oligomeric Silsesquioxane Copolymers. *Macromolecules* **2002**, *35*, 2375−2379.
(63) Leu, C. M.; Chang, Y. T.; Wei, K. H. Synthesis and Dielectric Properties of Polyimide-Tethered Polyhedral Oligomeric Silsesquioxane (POSS) Nanocomposites via POSS-diamine. *Macromolecules* **2003**, *36*, 9122−9127.
(64) Zheng, L.; Hong, S.; Cardoen, G.; Burgaz, E.; Gido, S. P.; Coughlin, E. B. Polymer Nanocomposites through Controlled Self-Assembly of Cubic Silsesquioxane Scaffolds. *Macromolecules* **2004**, *37*, 8606−8611.
(65) Gebald, C.; Wurzbacher, J. A.; Tingaut, P.; Zimmermann, T.; Steinfeld, A. Amine-Based Nanofibrillated Cellulose As Adsorbent for CO_2 Capture from Air. *Environ. Sci. Technol.* **2011**, *45*, 9101−9108.
(66) Danon, A.; Stair, P. C.; Weitz, E. FTIR Study of CO_2 Adsorption on Amine-Grafted SBA-15: Elucidation of Adsorbed Species. *J. Phys. Chem. C* **2011**, *115*, 11540−11549.
(67) Srikanth, C. S.; Chuang, S. S. C. Infrared Study of Strongly and Weakly Adsorbed CO_2 on Fresh and Oxidatively Degraded Amine Sorbents. *J. Phys. Chem. C* **2013**, *117*, 9196−9205.
(68) Bacsik, Z.; Ahlsten, N.; Ziadi, A.; Zhao, G.; Garcia-Bennett, A. E.; Martin-Matute, B.; Hedin, N. Mechanisms and Kinetics for Sorption of CO_2 on Bicontinuous Mesoporous Silica Modified with *n*-Propylamine. *Langmuir* **2011**, *27*, 11118−11128.
(69) Sayari, A.; Gorji, A. H.; Yang, Y. CO_2-Induced Degradation of Amine-Containing Adsorbents: Reaction Products and Pathways. *J. Am. Chem. Soc.* **2012**, *134*, 13834−13842.

DOI: 10.1021/acsami.5b04674
ACS Appl. Mater. Interfaces 2015, 7, 17969−17976